RESEARCHERID
THOMSON REUTERS

[Arezoo* *et al.*, 6(6): June, 2017]
IC™ Value: 3.00

ISSN: 2277-9655
Impact Factor: 4.116
CODEN: IJESS7

IJESRT

INTERNATIONAL JOURNAL OF ENGINEERING SCIENCES & RESEARCH TECHNOLOGY

OPTIMIZATION OF CARBIDE BALL NOSE END MILL PROFILE ANGLES IN MACHINING INCONEL 718

Ghasem Esmati, Behrooz Arezoo*

* Department of Mechanical Engineering, Amirkabir University of Technology, Tehran, Iran

DOI: 10.5281/zenodo.809131

ABSTRACT

Cutting tools nearly make up 30% of all the manufacturing cost. Modeling and simulation of machining is essential for improving and increasing efficiency of the process. Inconel 718 alloy which is an iron-nickel based superalloy is widely used in rocket engines, turbine blades, molds and extrusion containers. The flute profile is the main part in the milling cutting tool body and has an important effect on the tool life and machining quality in milling processes. The flute profile includes rake, relief, helix and pitch angles. The conventional way of flute design, is based on trial and error which is costly and time consuming. In this article, the geometry of milling tool to obtain optimal angles which result in minimum force in machining of Inconel 718 are investigated. The design of experiments is carried out with Taguchi method and the analysis in Abaqus software for different cutting conditions with different spindle speed, feed rate, axial and radial depth of cut and profile geometries including rake angle, helix angle and relief angle. All the experiments are also analyzed with Advantedge software which shows a good compatibility between the results.

KEYWORDS: Optimization, Ball nose end mill flute profile, Taguchi method, Inconel 718

I. INTRODUCTION

The final form of many mechanical parts is produced by machining processes. In the final stage of bulk deformation processes such as forging, rolling and casting processes, material removal and machining is necessary to achieve the design dimensions and tolerances. Two of the main cutting processes are milling and turning, where the milling process is particularly important since usually there are no limitations in part shape and size.

Many researches are carried out to enhance the milling processes. The new analysis and simulation techniques are used in order to predict the milling tools and processes conditions without having to carry out expensive practical tests. One of the basic requirements in analysis and simulation of milling processes is the estimation and modeling of machining forces. Predicting and calculating the forces in the cutting operations is essential in evaluating machinability, wear and tool life, machining accuracy and surface roughness.

Inconel 718 superalloy (I 718) is a nickel-iron base superalloy whose compositions are shown in Table 1 [1]. Due to its price and availability and excellent mechanical properties at temperatures above 650°C, it is a standard alloy which is used for gas turbine disks and blades, molds and extrusion containers [2].

High Speed Steel cutting tools are versatile and economical for general purpose use. Powdered Metals HSS are operable under higher speed and produce longer tool life. However due to mechanical properties of I 718 only carbide and / or harder tools are used for machining operations [3].

Most of cutting tool producers provide their tools for machining a wide range of materials with different machining conditions. As a result, these companies recommend tools with a specific profile for machining several types of materials which makes the optimum tool selection very difficult. In the present work the optimized profile for minimizing machining forces for dry milling of Inconel 718 with uncoated ball nose end mill is studied using finite element analysis.

Ozel et al. [4] investigated three-dimensional finite element modeling of chip formation process for machining I 718 where they compared the predictions of Abaqus and Deform finite element softwares.

Hortig and Svendsen [5] investigated the simulation of chip formation during high-speed cutting and showed that there are high correlations between the size and orientation of the elements used in analysis and the resulted forces and chip geometry. Kobayashi et al. [6] investigated the plastic flow behavior of I 718 under dynamic shear loads. The output of their research was the determination of the parameters of Johnson-Cook model and constitutive model of materials that

can be used in finite element simulation. Ozel and Ulutan 7**] [** investigated the prediction of machining induced residual stresses in turning of titanium and nickel based alloys with experiments and finite element simulations. They discussed the effect of tool paramaters such as tool edge radius and coating on the resulting stress profile. Their results are useful in prediction of machined surface integrity. Surface integrity is critical in fatigue life of titanium and nickel parts. Soo et al. [8] investigated the three dimensional finite element modeling of machining I 718 and suggested prelinimary actions for simulation of ball nose end mill. Uhlmann et al. [9] carried out two and three dimensional machining simulation of I 718 using finite element analysis, the results of which showed a good agreement with experimental tests. Ulutan and Ozel [10] published a review paper regarding machining induced surface integrity in titanium and nickel alloys.

In the present work the profile optimization of ball nose end mill is carried out. The Johnson-Cook damage and constitutive model for finite element simulation is used. These models which were introduced by Johnson and Cook [11, 12] are used by many researchers to study the behavior of materials.

Ball nose end mills (Figure 1) are widely used in milling operations. Positive rake angles improve cutting conditions and reduce machining forces. However it weakens the cutting edge and increases the probability of tool failure. High helix angle lead to more process uniformity and reduce the tool impact force when entering the contact area [13]. In this paper down-milling of I 718 without any coolant (dry) is studied.

Table 1 Chemical composition of Inconel 718 superalloy

ISSN: 2277-9655
Impact Factor: 4.116
CODEN: IJESS7

Co	Cr	Co+Ni	S	P	Si	Mn	C	%
---	17	50	---	---	---	---	---	Min
1	21	55	0.015	0.015	0.35	0.35	0.08	Max
	Fe	Ta+Nb	Cu	B	Ti	Mo	Al	%
	Balance	4.75	---	0.001	0.65	2.8	0.35	Min
	Balance	5.5	0.15	0.006	1.15	3.3	0.8	Max

Fig. 1 Ball Nose end mill

II. MATERIALS AND METHODS

The process parameters

Johnson-Cook constitutive model illustrates the effects of strain hardening, strain rate and thermal softening in yielding stress. Equation No. 1 shows this relationship [11].

$$\sigma = [A + B\varepsilon^{n}][1 + C\, ln\, \dot{\varepsilon}^{*}][1 - T^{*m}] \quad (1)$$

Where σ is flow stress tensile Von-Mises, ε is plastic strain equivalent, $\dot{\varepsilon}^{*} = \frac{\dot{\varepsilon}}{\dot{\epsilon}_0}$ is strain rate plastic dimensionless, $\dot{\varepsilon}$ is strain rate, $\dot{\epsilon}_0$ is strain rates, $T^{*} = \frac{T - T_{room}}{T_{melt} - T_{room}}$ is homologous temperature, T is temperature, T_{room} is room temperature, T_{melt} is melting temperature, and A, B, C, n and m are material constants .

Johnson-Cook damage model illustrates the effects of strain hardening, strain rate and thermal softening in fracture strain. Equation No. 2 shows this relationship [12].

$$\varepsilon^{f} = \left[D_1 + D_2 e^{D_3 \sigma^{*}}\right][1 + D_4 \ln \dot{\varepsilon}^{*}][1 + D_5 T^{*}] \quad (2)$$

Where ε^{f} is fracture strain, $\sigma^{*} = \frac{\sigma_m}{\bar{\sigma}}$ is dimensionless pressure-stress with the condition $\sigma^{*} \leq 1.5$, σ_m is the average of the three normal stresses, $\bar{\sigma}$ is the Von-Mises equivalent stress, and D_1, D_2, D_3, D_4 and D_5 are material constants.

In this paper, the workpiece which is I 718 is machined with H10F carbide tool. Material characteristics of workpiece are given in Table 2[14]. In this Table, E is Young's modulus, υ is Poisson's ratio, ρ is the density, c_p is specific heat capacity, χ is inelastic heat fraction, T_r is room temperature and T_m is the melting temperature.

Table 2 Physical and mechanical properties of Inconel 718 superalloy

C	n	B	A	χ	c_p	ρ	υ	E	
---	---	MPa	MPa	---	J/kg°C	Kg/m^3	---	GPa	Unit
0.006	0.54	1284	1200	0.9	435	8190	0.33	185	Amount
D_5	D_4	D_3	D_2	D_1	T_m	T_r	m	$\dot{\epsilon}_0$	
---	---	---	---	---	°C	°C	---	s^{-1}	Unit
0.89	0.04	-1.45	0.75	0.11	1800	25	1.2	0.001	Amount

ISSN: 2277-9655
Impact Factor: 4.116
CODEN: IJESS7

Material characteristics of carbide tool (H10F) are given in Table 3[15].

Table 3 Physical and mechanical properties of H10F-Carbide Tool

Amount	unit	Property
580	GPa	E
0.22	---	υ
14500	Kg/m^3	ρ

3. Design of Experiments with Taguchi method

In the present work Taguchi method is used for design of the experiments. The cutting force is being optimized with regards to geometry of ball nose end mill flute angles (radial rake angle, helix angle, radial relief angle) and cutting conditions.The range of angles and cutting conditions used in the optimization process are obtained through well-known cutting tool manufacturers such as Sandvik and Guhring.

The mentioned angles are studied at four different levels. As a result, a L16 orthogonal matrix is constructed. Three different levels for each machining conditions are considered and experiments are repeated for all levels. So there are 16 experiments for any level of machining conditions and a total of 48 experiments. Machining conditions include feed rate, cutting velocity, radial depth of cut and axial depth of. In this work the coefficient of friction is considered as an item dependant on cutting velocity [17]. Minitab software for the Taguchi method is used. Tables 4 and 5 illustrate the optimization tests and the machining conditions levels which are used in optimization tests respectively.

Table 4 Optimization tests

Radial relief angle (degree)	Helix angle (degree)	Radial rake angle (degree)	Test No.		
0	30	0	33	17	1
5	40	0	34	18	2
10	50	0	35	19	3
15	60	0	36	20	4
5	30	5	37	21	5
0	40	5	38	22	6
15	50	5	39	23	7
10	60	5	40	24	8
10	30	10	41	25	9
15	40	10	42	26	10
0	50	10	43	27	11
5	60	10	44	28	12
15	30	15	45	29	13
10	40	15	46	30	14
5	50	15	47	31	15
0	60	15	48	32	16

Table 5 Machining conditions in optimization tests

Friction coefficient (-)	Axial depth of cut (mm)	Radial depth of cut (mm)	Feed per tooth (mm/tooth)	Spindle speed (rpm)	Test No.
0.4	1.2	3.2	0.02	795.77	1-16
0.3	1.6	4	0.03	1591.55	17-32
0.2	2	4.8	0.04	2387.32	33-48

Ball end mill with diameter of 8 mm is considered in this study. In addition, in order to reduce the numerical calculations, only 10 mm length of the tool has been considered.

ISSN: 2277-9655
Impact Factor: 4.116
CODEN: IJESS7

4. Finite element simulations in Abaqus and Advantedge softwares

In the present work all experiments are analyzed with Abaqus software the results of which are verified by Advantedge software. Since Abaqus is more comprehensive software, therefore one of the goals of this research is to use Abaqus for simulation instead of using expensive special purpose softwares such as Advantedge.

All analysis is performed in three dimensions on Corei7 platform. Due to complexity of the geometry of end mills, they are modeled by Solidworks software and exported to Abaqus explicit. Also for simplicity, two Flute end mill is studied in the present work.

III. RESULTS AND DISCUSSION

Results of simulation with Abaqus and Advantedge software

Multiple outputs can be extracted from analytical software which can be used according to the requirements. After executing all experiments in Abaqus and Advantedge softwares, tool forces are studied. The maximum tool force (indicated by the symbols max) and average tool force (indicated by the symbol ave) are calculated by both softwares and presented in Table 6. The error percentage of Abaqus compared with Advantedge software is calculated by Equation 3:

$$\text{Error}\% = \frac{F_{Abq} - F_{Adv}}{F_{Adv}} \times 100 \quad (3)$$

Where F_{Abq} and F_{Adv} are the forces calculated by Abaqus and Advantedge respectively. As can be seen in Table 6, the errors are less than 5%.

Table 6 Force results in milling simulation with Abaqus and Advantedge softwares

%Second error	$F_{Adv,ave}$(N)	$F_{Abq,ave}$(N)	% First error	$F_{Adv,max}$(N)	$F_{Abq,max}$(N)	Run No.
1.836682	4926.669243	5017.156483	4.934436108	21207.21507	22253.67155	1
0.722232	360.550685	363.1546982	-3.65594115	1005.896989	969.1219873	2
-3.46548	410.3780737	396.1564965	-2.119931328	916.5926262	897.161492	3
-3.79635	329.9922331	317.4645653	-2.058352375	726.9472607	711.9841245	4
0.472085	306.7118071	308.1597463	-1.039032387	687.2614634	680.1205942	5
1.024702	4862.626084	4912.453531	4.472625268	24505.10351	25601.12496	6
-1.65528	226.7082981	222.9556498	4.206978426	502.9985411	524.1595812	7
2.309519	147.6450883	151.0549803	4.414297666	378.4490532	395.1549209	8
1.306889	375.1056974	380.0079125	2.451306351	595.5560508	610.1549541	9
4.097032	270.0936626	281.1594873	-4.488965557	533.0535412	509.1249513	10
1.629732	4817.611334	4896.125498	-3.288435237	24446.10998	23642.21549	11
-2.79452	246.0729711	239.1964023	4.065613504	629.5303282	655.1245982	12
-4.27721	311.7717449	298.4366108	3.454022393	554.9571506	574.1254949	13
2.326819	362.480046	370.9142997	2.922263907	612.5592216	630.4598186	14
0.445259	285.717894	286.990079	2.691970462	679.8239279	698.1245872	15
1.029709	4663.984397	4712.009843	-4.978024436	25444.77181	24178.12485	16
1.970908	5891.032011	6007.138821	-4.17407474	23523.06921	22541.19872	17
-3.35308	491.5904088	475.1069722	-4.426315032	964.8798262	922.1712054	18
3.57411	495.4162325	513.1229533	4.188899588	980.4922876	1021.564125	19
1.139473	376.7163417	381.0089241	-2.936094865	986.0737146	957.1216549	20
4.837783	534.2643744	560.1109247	-4.727002196	1217.099477	1159.567158	21
-4.21711	5852.582947	5605.773163	3.932690186	27083.85023	28148.97415	22
1.71185	386.1120222	392.72168	-4.110027586	885.9749756	849.5611597	23
0.394013	429.1104591	430.8012098	-4.832903623	949.4008173	903.5171908	24
3.089513	507.7745204	523.4622781	3.990553477	937.1225349	974.5189108	25
1.864414	424.8938812	432.8156642	-4.98443265	959.3133493	911.4970215	26
-1.76856	5413.518034	5317.776548	-4.351488038	28232.0282	27003.51487	27
4.141941	383.2926838	399.1684422	-4.645018922	901.4126682	859.5418792	28
-1.89734	460.6954046	451.9544626	0.735523698	845.00032	851.2154976	29

ISSN: 2277-9655
Impact Factor: 4.116
CODEN: IJESS7

-3.4256	349.9421911	337.9545877	-4.554989826	562.7900153	537.1549874	30
-3.31731	453.150416	438.117998	4.946302081	780.8372425	819.4598112	31
-2.94087	5354.720131	5197.244689	4.192435607	24133.35075	25145.12594	32
-4.77147	6786.988017	6463.148672	-4.636354643	26527.39932	25297.49501	33
4.601937	671.5934442	702.4997531	-2.075826002	1404.305899	1375.154952	34
1.905987	649.1260176	661.4982771	4.308355077	1512.945361	1578.12842	35
-2.39731	467.1905279	455.9905422	0.1869776	1276.615564	1279.002549	36
3.664554	743.3996565	770.6419351	-3.80171247	1486.216184	1429.714518	37
-4.19273	6650.328495	6371.498002	-4.335076964	26215.61979	25079.1525	38
-1.81754	594.2988457	583.4972546	-1.847694747	1613.947278	1584.126458	39
0.822629	520.6180108	524.9007662	-2.927778233	1275.867544	1238.512972	40
-3.0008	705.6193291	684.4451028	4.046273917	1517.541305	1578.945183	41
-4.35205	638.6368771	610.843052	2.701329168	1525.28654	1566.48955	42
4.531792	6328.975221	6615.791201	-0.36070204	23081.76791	22998.5115	43
-1.46148	530.0405546	522.2941058	-2.698334892	1349.670536	1313.251905	44
1.524868	718.8846861	729.8467291	-3.153809523	1758.988119	1703.512984	45
1.958113	654.9851818	667.8105295	1.430963445	1285.727687	1304.12598	46
3.759564	601.488107	624.1014392	2.867685946	1239.115568	1274.649511	47
-4.42297	6117.75329	5847.166842	1.758934486	17810.21962	18123.48972	48

6. Optimization Results

In the present work optimization is done on the average of the tool force and Minitab software is used with the Taguchi method. In the analysis of S/N (signal to noise ratio) signal is used for the output characteristic desired effect and noise is used for the output characteristic undesired effect. Signal to noise ratio reflects the sensitivity of the quality characteristics of case study to effective output and uncontrollable factors in a controlled process. In the Taguchi method this concept is used to obtain optimum conditions in the experiments. In experiments with repetition, the variance index is used which is also known as signal to noise ratio. The larger the value of S/N, the variance around the characteristic value will be smaller. Signal to noise ratio for quality characteristics with smaller value is better. The S/N can be calculated as in Equation No. 4 [16]. In these experiments, the goal is to find the highest S/N in the results. The higher S/N indicates that the effect of controllable parameters are more than uncontrollable or disturbance parameters. Production process design with the highest signal to noise ratio creates the most optimal quality with minimal variance. S/N curves for experiments 1-16, 17-32 and 33-48 are shown in Figures 2, 3 and 4.

$$\frac{S}{N} = -10\log_{10}\left[\frac{1}{n}\left(\sum_{i=1}^{i=n} y_i^2\right)\right] \quad (4)$$

Where n is the number of experiment and y_i is the result of any run in the experiment.

ISSN: 2277-9655
Impact Factor: 4.116
CODEN: IJESS7

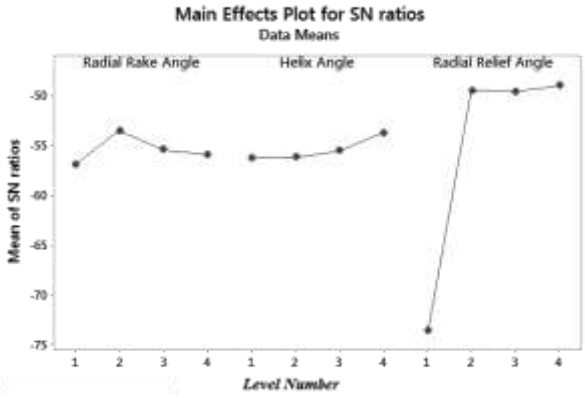

Fig.2S/N ratio curves for experiment 1-16

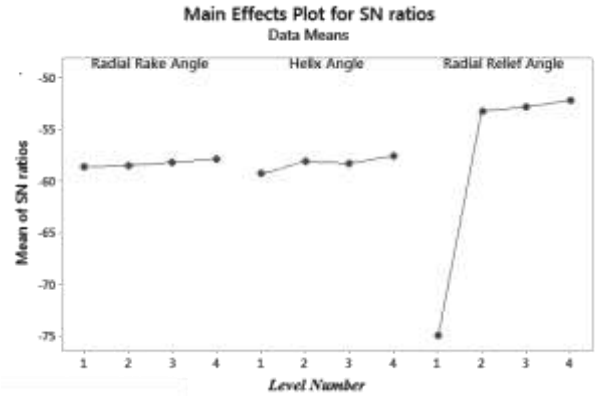

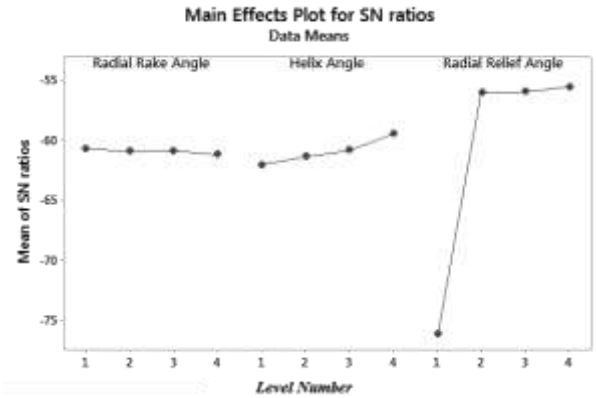

Fig.4S/N ratio curves for experiment 33-48

Considering figures 2 to 4, it is obvious that the fourth level of the two variables radial relief angle and helix angle leads to the highest signal to noise ratio. As shown in these Figures, the highest signal to noise ratio of the radial rake angle depends on the machining conditions. In experiments 1-16, 17-32 and 33-48 the highest signal to noise ratio is obtained at the levels of 4, 2 and 1. Because the non-uniformity of optimal solution for radial rake angle in different experiments, it is necessary to perform additional experiments individually in experiments 1-16, 17-32 and 33-48 for all three levels. In these experiments fourth level of radial rake angle and helix angle will be considered. Because the experiments 4, 20 and 36 which were carried out before, contained the first level of radial rake angles, so here six complementary experiments are carried out. Two experiments exist with level 2 and 4 of radial rake angle and level 4 of radial relief angle and helix angle for any machining condition. List of 6 complementary experiments and calculated forces with Advantedge software is given in Table 7. By comparing the force results in tables 6 and 7 for each machining condition levels with previous results it can be observed that minimum force is the force mentioned in table 6. As shown in Figures 5 to 7,

ISSN: 2277-9655
Impact Factor: 4.116
CODEN: IJESS7

when the radial relief angle is equal to zero the force is very large and therefore this angle is not permitted. A minimum of 3 degrees for radial relief angle is suggested for reducing forces. It should be noted that when the experiment contains repetition in any experiment step, the signal to noise ratio is the best choice for calculation and controlling the effect of total deviation of average value from goal value [16]. So here the analysis of variance is used and the answer is considered as an optimal solution. The aim of the present work is to presents end mill profiles which result in minimum tool force in different machining conditions. Thus, according to performed experiments force can be assumed an independent parameter at any level of machining conditions and perform minimizing those parameters. This means there are 16 experiments which obtain three type of force. By optimizing these parameters the tool geometry that represents the minimum forces at different machining conditions are obtained. One of the methods used for optimization is Grey relational analysis [18]. Grey method is applied for converting multi-objective optimization problem to single-objective optimization problem. The first step in Grey method is normalization of obtained results with respect to desirable response. So the forces are normalized according to Equation No. 5. These results are given in table 8.

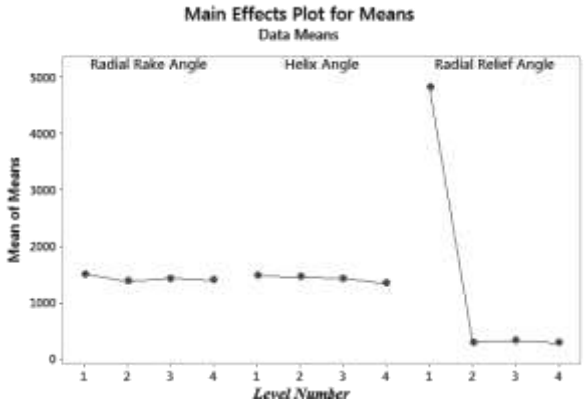

Fig.5 Mean force curves for experiment 1-16

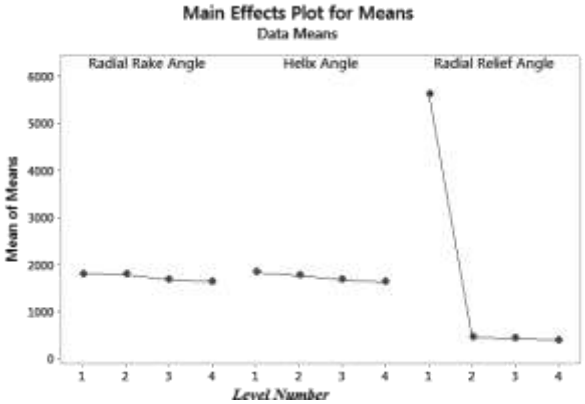

Fig.6 Mean force curves for experiment 17-32

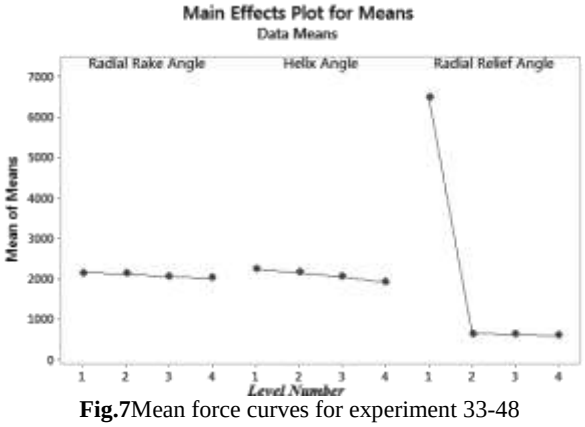

Fig.7 Mean force curves for experiment 33-48

ISSN: 2277-9655
Impact Factor: 4.116
CODEN: IJESS7

$$x_i^*(k) = \frac{\max\left(x_i^0(k)\right) - x_i^0(k)}{\max\left(x_i^0(k)\right) - \min(x_i^0(k))} \quad (5)$$

Where$x_i^*(k)$, is the result value after normalization, $\max\left(x_i^0(k)\right)$ and $min\left(x_i^0(k)\right)$ are maximum and minimum values of $x_i^0(k)$ for k'th response respectively, where k is equal to 1, 2 and 3 for force results at levels 1, 2 and 3.

Table 7 Complementary Optimization tests

Force(N)	Machining condition level	Radial relief angle (degree)	(degree) Helix angle	(degree) Radial rake angle	Run No.
155.5392023	1	15	60	5	49
208.8392034	1	15	60	15	50
261.7147268	2	15	60	5	51
275.2156541	2	15	60	15	52
406.3595606	3	15	60	5	53
392.7529068	3	15	60	15	54

Table 8 Normalized experimental results

F_3	F_2	F_1	Experiment No.
0	0	0	1
0.967657	0.974437	0.95545	2
0.971212	0.973746	0.945024	3
1	0.995168	0.961844	4
0.956295	0.966735	0.966716	5
0.021624	0.006939	0.013401	6
0.979887	0.993472	0.983456	7
0.991546	0.985713	1	8
0.962273	0.971516	0.952404	9
0.972872	0.986473	0.974378	10
0.072473	0.086177	0.02282	11
0.990055	0.993981	0.979404	12
0.960174	0.980012	0.965657	13
0.970285	1	0.955046	14
0.97875	0.981374	0.971109	15
0.105895	0.096788	0.054966	16

Now Grey relational coefficients ($\xi_i(k)$) shall be created through equations 6 to 9. These coefficients express the relationship between the actual results of the experiments and the ideal results. These results are given in Table 9.

$$\xi_i(k) = \frac{\Delta_{min} + \xi\Delta_{max}}{\Delta_{0i}(k) + \xi\Delta_{max}} \quad (6)$$

$$\Delta_{0i}(k) = |x_0^*(k) - x_i^*(k)| \quad (7)$$

$$\Delta_{min} = \min_{\forall j \in i} \min_{\forall k} |x_0^*(k) - x_j^*(k)| \quad (8)$$

ISSN: 2277-9655
Impact Factor: 4.116
CODEN: IJESS7

$$\Delta_{max} = \max_{\forall j \in i} \max_{\forall k} \left| x_0^*(k) - x_j^*(k) \right| \quad (9)$$

In equations 6 to 9 $\Delta_{0i}(k)$ is deviation sequence from reference sequence $x_0^*(k)$ and comparability sequence $x_i^*(k)$.
Distinguishing coefficient (ξ) is a number between 0 and 1 and is used in order to adjust the difference between relational coefficients. In this work ξ is assumed 0.5. Grey relational grade ($\propto_i$) calculated by equation No. 10.

$$\propto_i = \frac{1}{n} \sum_{k=1}^{k=n} \xi_i(k) \quad (10)$$

Table 9 Grey relational coefficients

F_3	F_2	F_1	Experiment No.
0.333333	0.333333	0.333333	1
0.939244	0.95136	0.918189	2
0.945558	0.950112	0.900939	3
1	0.990429	0.929099	4
0.919616	0.937621	0.937586	5
0.338209	0.334882	0.336338	6
0.96133	0.987113	0.967972	7
0.983373	0.972219	1	8
0.929839	0.946102	0.913083	9
0.948535	0.97366	0.951254	10
0.350256	0.353651	0.338483	11
0.980498	0.988106	0.960438	12
0.926224	0.961561	0.935728	13
0.943903	1	0.917509	14
0.959232	0.964086	0.945374	15
0.358653	0.356325	0.346013	16

In equation No. 10 n is the number of performance characteristics. Greater Grey relational grade result in convergence of experiment results to ideal results. So the greater Grey relational grade shows convergence of parameters collection to optimal results. The final step is sorting the Grey relational grade in descending order which can be seen in Table 10 and illustrated in Figure 8.

Table 10 Grey relational grade and its order

Order	Grade	Experiment No.
16	0.333333	1
9	0.936264	2
10	0.932203	3
3	0.973176	4
11	0.931608	5
15	0.336477	6
4	0.972138	7
1	0.985197	8
12	0.929675	9
5	0.957816	10
14	0.347463	11
2	0.976347	12
8	0.941171	13
7	0.953804	14
6	0.956231	15
13	0.353664	16

ISSN: 2277-9655
Impact Factor: 4.116
CODEN: IJESS7

In table 8, F_1, F_2 and F_3 are forces which are obtained in miscellaneous machining conditions where the machining conditions of experiments No. 1-16, 17-32 and 33-48 are shown in Table 5. Greater normalized result means better performance where in the best performance the normalized result is equal to 1.
According to Table 10 and Figure 8 the optimal combination to achieve the lowest force by a tool are radial rake angle of 5 degrees, helix angle of 60 degrees and radial relief angle of 10 degrees.

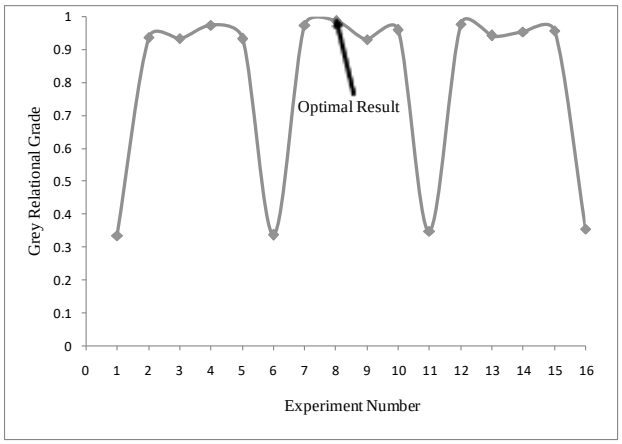

Fig.8 Grey relational grade

IV. CONCLUSION

Appropriate tool selection is an important factor in machining of materials. Most of cutting tool producers provide their tools for machining a wide range of materials with different machining conditions. As a result, these companies recommend tools with a specific profile for machining several types of materials which makes the optimum tool selection very difficult. In the present work the optimized profile for minimizing machining forces for dry milling of Inconel 718 with uncoated ball nose end mill is presented. It is observed that machining forces are decreased with increasing radial relief angle and helix angle. In the present work the optimal combination to achieve the lowest force by a tool are found to be with radial rake angle of 5 degrees, helix angle of 60 degrees and radial relief angle of 10 degrees. It is shown that Abaqus software has acceptable accuracy in simulation of milling processes and obtains reasonable results which are in good agreement with Advantedge software.

V. REFERENCES

[1] E. O. Ezugwu, Z. M. Wang, A. R. Machado, The machinability of nickel-based alloys: a review, Journal of Materials Processing Technology, Vol. 86, No. 1, pp. 1-16, 1999.
[2] C. T. Sims, N. S. Stoloff, W. C. Hagel, S. Ii, High-temperature materials for Aerospace and industrial Power, A Wiley-Interscience, 1987.
[3] J. G. Corrêa, R. B. Schroeter, Á. R. Machado, Tool life and wear mechanism analysis of carbide tools used in the machining of martensitic and supermartensitic stainless steels, Tribology International, Vol. 105, pp. 102-117, 2017.
[4] T. Ozel, I. Llanos, J. Soriano, P. J. Arrazola, 3D finite element modelling of chip formation process for machining Inconel 718: comparison of FE software predictions, Machining Science and Technology, Vol. 15, No. 1, pp. 21-46, 2011.
[5] C. Hortig, B. Svendsen, Simulation of chip formation during high-speed cutting, Journal of Materials Processing Technology, Vol. 186, No. 1, pp. 66-76, 2007.
[6 T. Kobayashi, J. W. Simons, C. S. Brown, D. A. Shockey, Plastic flow behavior of Inconel 718 under dynamic shear loads, International Journal of Impact Engineering, Vol. 35, No. 5, pp. 389-396, 2008.
[7] T. Özel, D. Ulutan, Prediction of machining induced residual stresses in turning of titanium and nickel based alloys with experiments and finite element simulations, CIRP Annals-Manufacturing Technology, Vol. 61, No. 1, pp. 547-550, 2012.
[8] S. L. Soo, D. K. Aspinwall, R. C. Dewes, 3D FE modelling of the cutting of Inconel 718, Journal of Materials Processing Technology, Vol. 150, No. 1, pp. 116-123, 2004.
[9] E. Uhlmann, M. G. von der Schulenburg, R. Zettier, Finite element modeling and cutting simulation of Inconel 718, CIRP Annals-Manufacturing Technology, Vol. 56, No. 1, pp. 61-64, 2007.
[10 D. Ulutan, T. Ozel, Machining induced surface integrity in titanium and nickel alloys: a review, International Journal of Machine Tools and Manufacture, Vol. 51, No. 3, pp. 250-280, 2011.
[11]G. R. Johnson, W. H. Cook, A constitutive model and data for metals subjected to large strains, high strain rates and high temperatures, in Proceeding of, The Hague, The Netherlands, pp. 541-547.
[12]G. R. Johnson, W. H. Cook, Fracture characteristics of three metals subjected to various strains, strain rates, temperatures and pressures, Engineering fracture mechanics, Vol. 21, No. 1, pp. 31-48, 1985.
[13]M. Yang, H. Park, The prediction of cutting force in ball-end milling, International Journal of Machine Tools and Manufacture, Vol. 31, No. 1, pp. 45-54, 1991.

[14]B. Erice Echávarri, Flow and fracture behaviour of high performance alloys, Thesis, Caminos, 2012.
[15]J. W. X. McCauley, Ceramic armor materials by design: American Ceramic Society USA, 2002.
[16] R. K. Roy, A primer on the Taguchi method. Competitive manufacturing series, New York, pp. 7-80, 1990.
[17] F. Zemzemi, J. Rech, W. B. Salem, A. Dogui, P. Kapsa, Identification of friction and heat partition model at the tool-chip-workpiece interfaces in dry cutting of an Inconel 718 alloy with CBN and coated carbide tools, Advances in Manufacturing Science and Technology, Vol. 38, No. 1, 2014.
[18]D. Julong, Introduction to grey system theory, The Journal of grey system, Vol. 1, No. 1, pp. 1-24, 1989.

CITE AN ARTICLE

Esmati, G., & Arezoo, B. (2017). OPTIMIZATION OF CARBIDE BALL NOSE END MILL PROFILE ANGLES IN MACHINING INCONEL 718. *INTERNATIONAL JOURNAL OF ENGINEERING SCIENCES & RESEARCH TECHNOLOGY*, *6*(6), 245-256. doi:10.5281/zenodo.809131